Probiotics enhance susceptibility of mice to cryptosporidiosis

5   Bruno C. M. Oliveira[1,2] and Giovanni Widmer[2]*

[1]Universidade Estadual Paulista (UNESP), Faculdade de Medicina Veterinária, Araçatuba, Brazil.

[2]Cummings School of Veterinary Medicine at Tufts University, North Grafton, Massachusetts,
10 USA.

One Sentence Summary: Mice treated with probiotics develop more severe symptoms of cryptosporidiosis.

Abstract: Cryptosporidiosis is a leading cause of diarrhea in infants and immune-compromised
15 individuals. The lack of effective drugs against this enteric infection is motivating research to develop alternative treatments. To this aim, the impact of probiotics on the course of cryptosporidiosis was explored. The native intestinal microbiota of specific pathogen-free immunosuppressed mice was initially depleted with orally administered antibiotics. Then, a commercially available probiotic product intended for human consumption was added (or not) to
20 the drinking water. Probiotic treated and untreated mice were orally infected with *Cryptosporidium parvum* oocysts. On average, mice treated with probiotic excreted more oocysts, indicative of a more severe infection. The probiotic treatment significantly altered the fecal microbiota, but taxonomic analyses showed no direct association between ingestion of probiotic bacteria and their abundance in fecal microbiota. These results suggest that probiotics
25 indirectly alter the intestinal microenvironment in such a way that favors proliferation of *C. parvum*. The increase in the relative abundance of facultative anaerobes observed in mice with severe cryptosporidiosis indicates that dysbiosis is a consequence of severe cryptosporidiosis. The increase in the abundance of facultative anaerobes observed in severely infected animals is consistent with analyses of microbiota from individuals infected with other enteric pathogens.

30   The results are significant because they show that *C. parvum* responds to changes in the

intestinal microenvironment induced by a nutritional supplement.

Introduction

Cryptosporidiosis is an enteric infection caused mostly by two species of *Cryptosporidium*

35   parasites, *C. parvum* and *C. hominis*. Transmission occurs when infectious oocysts are ingested,

either with contaminated food and water (*1, 2*), by fecal-oral contact and possibly by inhalation

(*3*). Recent surveys have revealed the high prevalence of cryptosporidiosis among infants living

in developing nations, where it causes substantial morbidity and mortality in infants less than 2

years of age. (*4*). The treatment of cryptosporidiosis is limited to supportive care since no

40   specific effective drugs available. Since no vaccines are available either, hygiene and water

sanitation to reduce transmission remain the most effective approaches.

Using experimental mouse infections, we previous showed that cryptosporidiosis changes

the gut microbiota. Given the importance of the microbiota to the physiology of the gut, here we

investigated whether a reverse effect, of the microbiota on the parasite, could be demonstrated.

45   We reasoned that the unmet need for anti-*Cryptosporidium* drugs could be alleviated by

probiotics. This hypothesis does not necessarily imply that the microbial community of the gut

directly impacts the parasite. Indeed, the transient nature of *Cryptosporidium* extracellular stages

limits interactions between the resident microbiota and cryptosporidial life stages including

sporozoites, merozoites and gametes. Alternatively, it is possible that the microbiota impacts

50   parasite proliferation by modulating epithelial defense mechanisms, impacting the protective

mucus layer, or stimulating innate and acquired immune cells.

The literature on the impact of the intestinal microbiota on cryptosporidiosis is sparse. A few studies have investigated the impact of *Cryptosporidium* parasites on the gut microbiota, but the effect of the gut environment on the course of the infection is not understood and the

55 underlying mechanisms are unknown. Using germ-free immunodeficient SCID mice compared to SCID mice colonized with intestinal microbes, Harp et al. showed that normal intestinal microbiota delayed the onset of *C. parvum* oocyst excretion by several weeks (*5*). These authors also showed that resistance of mice to *C. parvum* can be increased by transferring intestinal mucosa from resistant animals to susceptible infant mice (*6*). A protective role of the gut

60 microbiota against cryptosporidiosis was also observed in neonatal mice (*7, 8*). These authors found that gut microbiota synergized with poly(I:C) to elicit a protective intestinal immunity against *C. parvum*. A study on the effect of inosine monophosphate dehydrogenase inhibitors in *C. parvum* infected mice detected an increase in *C. parvum* virulence in response to the drug. This effect was attributed to an alteration of the intestinal microbiota (*9*).

65 Research with probiotics in animal models of other infectious diseases has generated diverging results. A mouse model of rotavirus infection was used to show that administration of *Lactobacillus reuteri* reduced the duration of diarrhea (*10*). Similarly, and consistent with what has been observed in human trials, probiotics administered to mice had a mitigating impact on colitis induced by *Citrobacter rodentium* (*11*). The significant public health impact of

70 nosocomial *Clostridium difficile* infection has generated a large body of research, including experiments in mice aimed at testing the benefit of fecal transplant (*12*) and defined probiotics (*13-15*). Only a few studies report a worse outcome with probiotic treatment. Using the cichlid fish tilapia, Liu et al. found that a 14-day treatment with probiotics made fishes more susceptible to infection with *Aeromonas hydrophila* after the treatment was discontinued (*16*). More relevant

75 to the present study, research with mice showed that supplementation of diet with kefir

exacerbated the outcome *Clostridium difficile* infection (*17*). Indicating that a harmful effect of

probiotics is unusual, no other studies in rodent or mammalian models demonstrating increased

susceptibility to infection appear to have been published.

  We previously reported a significant impact of cryptosporidiosis on the profile of the

80 bacterial intestinal microbiota (*18*). Replicated experiments with two *C. parvum* isolates

comprising two infected and two control groups of mice revealed that the intestinal microbiota of

infected animals differed from that of uninfected animals regardless of the *C. parvum* isolate. A

taxonomic analysis of bacterial taxa highlighted two unclassified Bacteroidetes operation

taxonomic unit (OTUs), Prevotellaceae and Porphyromonadaceae as overrepresented in the

85 feces of infected mice, whereas OTUs most over-represented in uninfected mice were classified

as Porphyromonadaceae and one unclassified Bacteroidetes OTU. With an eye on developing

alternative treatments, the experiments described here were aimed at assessing whether

probiotics can influence the course cryptosporidiosis. Although the results reveal a significant

trend for more severe infection, the results show that *C. parvum* proliferation responds to

90 changes in the intestinal microbiota. These observations open the way for targeted editing of the

intestinal microbiota (*19-21*) as a low-cost approach to reducing the impact of cryptosporidiosis.

Results

Probiotic increases severity of infection.

95 To test for a probiotic effect on the severity of *C. parvum* infection, fecal oocyst output was

measured by flow cytometry as described above. In experiment 1, a total of 92 oocyst

concentration values were acquired from 16 mice and six timepoints over a 15-day period. In

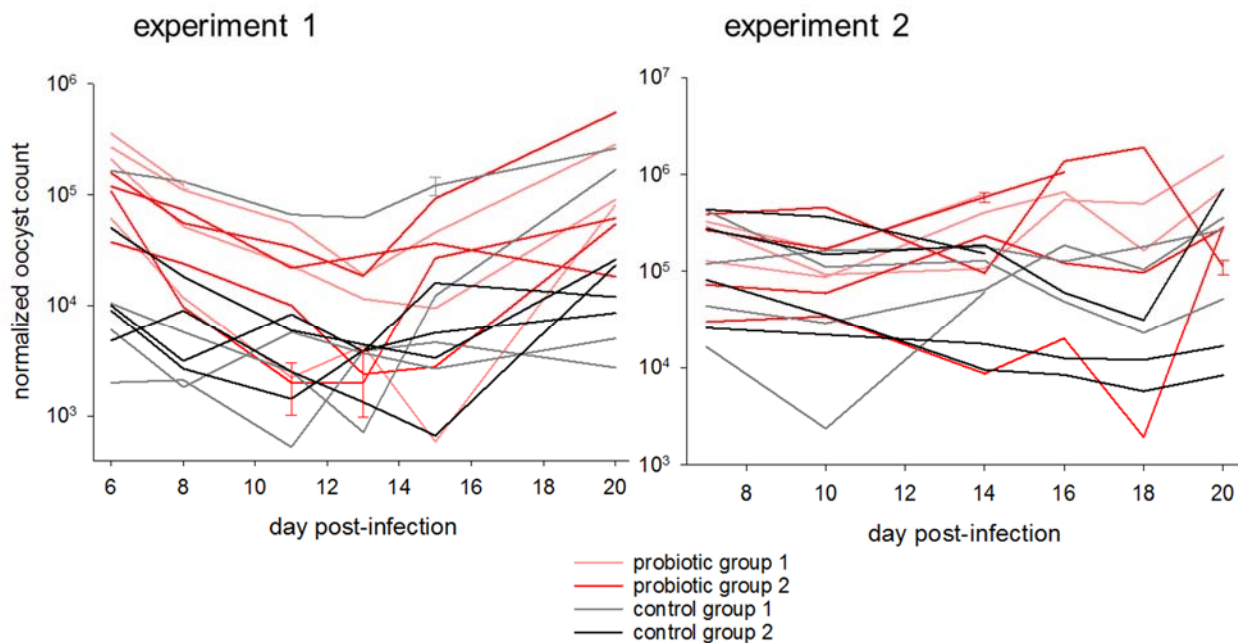experiment 2, 79 datapoints were obtained from the same number of mice (Fig. 1). In experiment

100   **Fig. 1** Effect of probiotic on severity of *C. parvum* cryptosporidiosis in immune-suppressed mice. The graphs show normalized oocyst counts expressed as oocysts/g feces for two independent experiments. Each line represents one mouse. Error bars show SD based on five replicate counts of selected samples.

105   1 mice which received probiotic excreted a significantly higher concentration of oocysts. A mean oocyst output of 76,463 oocysts/g feces (n=44) was measured against a mean of 26,732 oocysts/g for the control mice (n=48). The difference between treatments was highly significant (Mann-Whitney U=541, p<0.001). An analogous significant probiotic effect was obtained for experiment 2; $mean_{probiotic}$=378,736 oocysts/g, $n_{probiotic}$=37, $mean_{control}$=68,778 oocysts/g,

110    $n_{control}$=42; U=269.5, p<0.001). Fig. 1 shows the pattern of oocyst output for the two experiments plotted on a log scale. In experiment 1, due to early mortality and high oocyst output, the

concentration of dexamethasone in the water was lowered from 16 mg/l to 10 mg/l on day 8. This intervention is the likely cause of the reduction in oocyst output. Mouse mortality appeared to be unrelated to probiotic treatment, but the numbers are too small to support statistical testing.

115 In experiment 1, two mice out of 16 died during the experiment; one mouse from treatment group 1 on day 8 PI, and one mouse from control group 1 on day 15 PI. In experiment 2 two mice died, from treatment group 2 on day 16 PI and one from control group 1 on day 14 PI.

Probiotic treatment significantly impacts fecal microbiota.

120 To assess whether probiotic treatment impacted the fecal microbiota, pairwise weighted UniFrac distances (*22*) between sequence data from 64 experiment 1 fecal samples were visualized on a PCoA plot (Fig. 2). Samples collected starting on day 5 of probiotic treatment (day 4 PI) until day 16 of treatment (day 15 PI) were included. The number of samples in this analysis is smaller than shown in Fig. 1, because not all fecal samples were sequenced. Consistent with an impact of

125 probiotic consumption on the profile of the intestinal microbiota, this analysis revealed a non-overlapping distribution of datapoints according to treatment. ANOSIM was used to check the significance of sub-structuring by treatment. The test returned a highly significant *R* value of 0.305 ($p < 10^{-5}$). Analogous results were obtained for experiment 2 based on 55 samples collected starting on day 10 after probiotic treatment was initiated (day 9 PI) until day 20 (day 19 PI). As

130 for experiment 1, clustering by treatment was significant ($R = 0.210$, $p < 10^{-5}$).
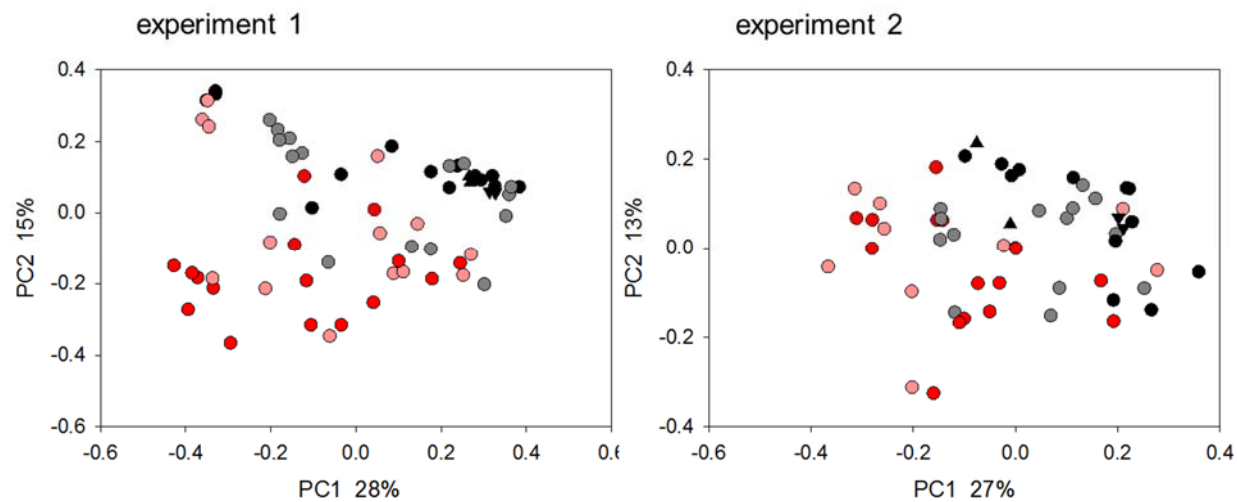
135

Fig. 2. Impact of probiotic on the fecal microbiome of *C. parvum* infected mice. Principal

Coordinate Analysis was used to display weighted UniFrac distances between pairs of fecal

microbiome samples. Experiment 1 analysis (left) includes data from 64 fecal samples

collected from day 5 of treatment (day 4 PI) until day 16 of treatment (day 15 PI). For

140 experiment 2, 55 samples were analyzed. Each datapoint represents one sample, color-coded

according to treatment and group as shown in Fig. 1. Matching triangle symbols indicate

replicate analyses of the same fecal samples.

Bacterial α-diversity does not correlate with oocyst output.

145 Having detected an impact of probiotic consumption on oocyst output and on the fecal

microbiota, the FCM and 16S data were analyzed jointly to identify possible associations

between bacterial microbiota profile and severity of cryptosporidiosis. These combined analyses

included all samples for which 16S and FCM data were acquired. A total of 44 samples were

included in each experiment. As dysbiosis is typically characterized by low bacterial diversity

150 and is often associated with increased susceptibility to enteric infections (*23*), the first global

analysis examined 16S sequence data and oocyst concentration for a possible correlation between microbiota α-diversity and total oocyst output (Fig. 3). Regardless whether all data were
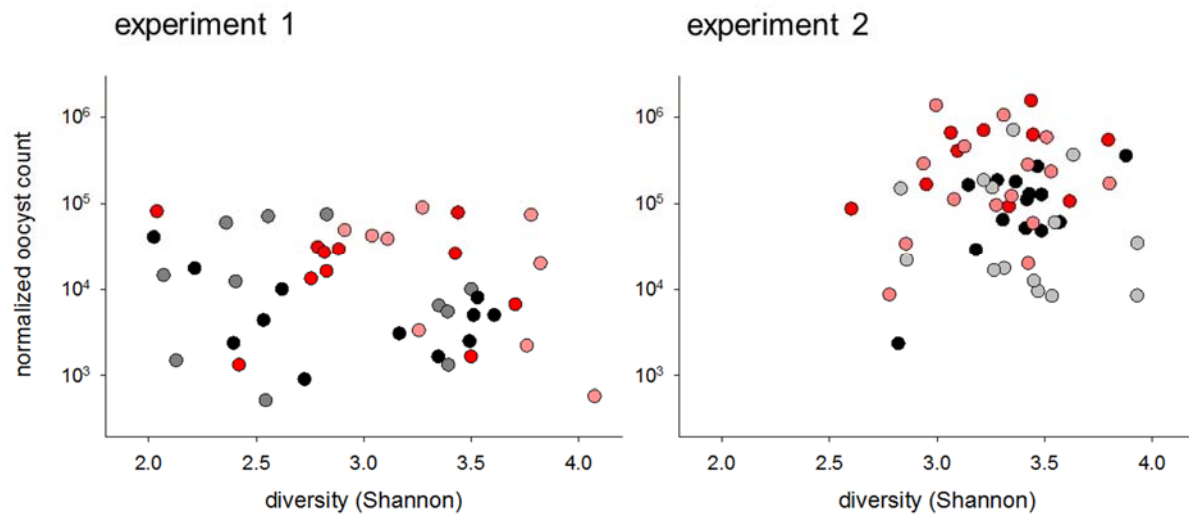

Fig. 3 Oocyst output is unrelated to diversity of bacterial microbiome. Oocyst output

155   normalized for feces volume was plotted against Shannon diversity for 44 samples collected

on three days which were analyzed for both properties in experiment 1 and 53 samples from

experiment 2. Color indicates experimental group as described in Fig. 1. Samples were

collected from individual mice.

160   pooled by experiment, or samples from probiotic treated and control mice were analyzed

separately, the correlation was very low, explaining 9% of oocyst output at most. If considering

only the 10 samples with the highest and lowest oocyst concentration (20 samples per

experiment), no correlation between oocyst output and α-diversity was apparent either. We also

used the Mantel test to assess whether the difference in oocyst output between pairs of samples

165   correlated with UniFrac distance. In other words, with this analysis we tested whether samples

harboring very different concentrations of oocysts also exhibited large phylogenetic distances.

No association between these variables was identified in either experiment (R_{xy}=0.12, n=44,

p=0.055 and Rxy=0.058, n=53, p=0.28) . Together with the results shown in Fig. 3, these

analyses indicate that higher oocyst output is not correlated with a global change in the

170   microbiota.

RDA was used as the second global analysis to assess whether fecal oocyst concentration

significantly correlated with microbiota profile and identifying bacterial OTUs correlating in

relative abundance with oocyst output. In experiment 1 a Monte Carlo test involving 1000

permutations of the 44 samples indicated a significant correlation between oocyst concentration

175   and OTU profile (pseudo-F=1.0, p=0.014). This effect remains significant (F=2.7, p=0.024) after

accounting for treatment, i.e., defining treatment (±probiotic) as covariate, or accounting for

"mouse" (defining mouse as covariate; pseudo-F=3.8, p=$6x10^{-5}$). The analogous test in

experiment 2 also returned a significant pseudo-F ratio of 4.2 (n=44, p=0.0016). If removing the

effect of treatment or "mouse" by defining each variable as covariate, the association remains

180   significant (pseudo-F=2.6; p=0.015 and pseudo-F=5.2; p=$3x10^{-4}$, respectively).

High abundance of facultative anaerobes in severe infections.

Having identified a significant correlation between fecal oocyst concentration and OTU profile,

the taxonomic make-up of the fecal microbiota was examined in more detail with the goal of

185   identifying bacterial taxa which correlate in abundance with oocyst output. First we used

program LEfSe (*24*) to identify OTUs which significantly define the difference between samples

containing high and low oocyst concentration. This analysis was based on 20 samples for each

experiment, 10 samples with the highest oocyst concentration and 10 samples with the lowest

concentration. In experiment 10, 7/10 samples in the high-oocyst group originated from mice

190   treated with probiotics and 7/10 samples in the low-oocyst group came from control mice (Chi-

square=3.2, p=0.07). In experiment 11, 9/10 samples in the high-oocyst group originated from

treated mice and 8/10 samples in the low-oocyst group originated from control mice (Chi-

square=9.9, p=0.002). Feces from highly infected animals were characterized by a high

Proteobacteria abundance, whereas feces from lightly infected animals were significantly

195   enriched for Firmicutes. As observed for the impact of the probiotic on the severity of

cryptosporidiosis (Fig. 1) and on the global microbiota profile (Fig. 2), a clear similarity was
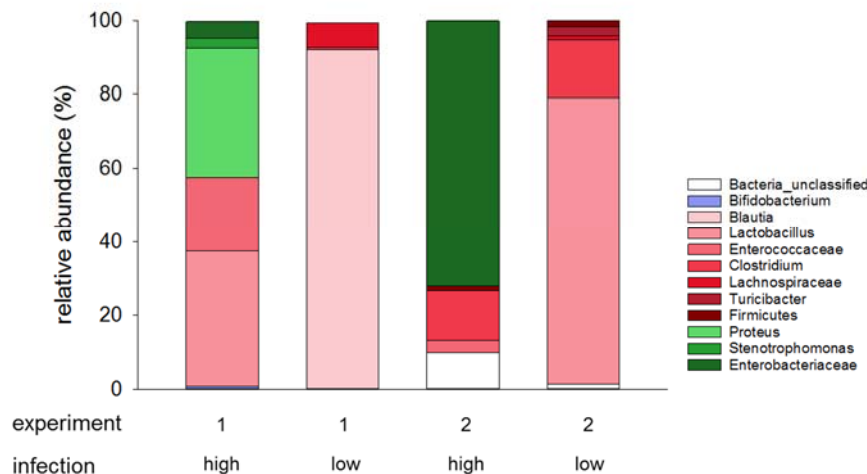
observed between the two experiments (Fig. 4).

Fig. 4 Taxonomy of fecal microbiome from heavily and lightly infected mice shows that

200   heavy infections are associated with increased abundance of Proteobacteria. For each

experiment, bacterial taxa significantly associated with severity of infection were identified

using LEfSe (24) in a comparison of ten samples with the highest (high) and lowest (low)

oocyst concentration; twenty samples were included for each experiment. Color indicates

phylum and color intensity genus or highest taxonomic level (family, order etc.) identified;

205   green Proteobacteria; red, Firmicutes; blue, Actinobacteria.

A second taxonomy analysis aimed at identifying OTUs enriched in highly infected animals was performed with RDA (*25*). For experiment 1, in the 10 OTUs which best correlated in relative abundance with oocyst concentration, 61% of the sequences were classified as Lactobacillus,

210   24% as Proteus and 14% as Enterococcus. In the 10 OTUs which most negatively correlated with oocyst concentration, as seen in with LEfSe, *Blautia* was the most abundant classification (61% of reads), followed by Clostridiaceae (27%), Lachnospiraceae (10%), Romboutsia (8%) and unclassified Firmicutes. For experiment 2, the identical analysis of the 10 OTUs which best correlated in relative abundance with oocyst concentration, 92% of sequences originated from

215   Enterobacteriaceae and 8% from Firmicutes. In the 10 OTUs with lowest oocyst concentration 70% of sequences were classified as Lactobacillus, 21% as Turicibacter, 6% as unclassified Lactobacillales and 1% as Stenotrophomonas (phylum Proteobacteria). The results obtained with RDA are thus is close agreement with the LEfSe results shown in Fig. 4.

220   *Severity of infection correlates with fecal microbiota profile across experiments.*
        Fig. 3 illustrates the main difference the experiments; mean fecal oocyst concentration across all time points, treatments and mice in experiment 2 was 2.4×10^5 oocysts/g (n=79, SD=3.4×10^5), or about 5 times higher than in experiment 1 (mean=5.0×10^4 oocysts/g, n=92, SD=8.7×10^4; Mann-Whitney U=1467, p<0.001). It is likely that this difference was caused by the different

225   routes of dexamethasone administration: drinking water only in experiment 1, vs. drinking water followed by IP injection in experiment 2. The more severe infection in experiment 2 represents an unplanned opportunity to further assess the impact of the infection on the gut environment. If heavier infections cause an increase in Proteobacteria relative abundance, as suggested by LEfSe

analysis (Fig. 4) and RDA described above, one would expect a higher proportion of

230   Proteobacteria in experiment 2 samples originating from severely infected mice, which is exactly

what was observed (Fig. 4 and RDA results). Further, severe cryptosporidiosis can be expected,

based on research on human patients suffering from other enteric infections (*26-28*), to lead to a

change in bacterial microbiota towards populations enriched for facultative anaerobes, possibly

resulting in less diversity. To test this hypothesis, mean pairwise weighted UniFrac distances

235   between microbiota from heavily infected samples were compared to distances between lightly

infected samples. In experiment 1, mean β-diversity between the 10 high-oocyst samples was

0.536 (45 pairwise distances, SD=0.142), whereas between low-output samples mean β-diversity

was 0.590 (45 pairwise distances, SD=0.121; Mann-Whitney T=1819.0, p=0.07). In experiment

2, the mean β-diversity values are 0.312 (45 pairwise distances, SD=0.117) and 0.411 (45

240   pairwise distances, SD=0.137) for the 10 samples with the highest and lowest oocysts

concentration, respectively (Mann-Whitney U=590, p<0.001). Although for experiment 1 the

effect is not significant, together these results are consistent with the model postulated above; i.e.

that severe infection leads to a convergence of the microbiota, towards an increase in the relative

abundance of Proteobacteria and a reduction in Firmicutes.

245

Loss of microbiota functional diversity in heavily infected mice.

To extend the observed taxonomic differences between severely and lightly infected mice to the

metagenome, program PICRUSt (*29*) was used to infer microbiota function from OTU profiles.

Given the more severe infection in experiment 2, metagenome analyses are only reported for this

250   experiment. PICRUSt identified 39 KEGG level 2 categories in the combined metagenome. A

PCoA based on pairwise SSR distance between KEGG abundance values normalized across

KEGG categories revealed a tight clustering of samples with high oocyst concentration relative to the samples with lower oocyst concentration (Fig. S1). This visual assessment was tested by comparing pairwise distances between KEGG profiles. For the ten samples with the lowest

255   oocyst concentration the distance averaged 69.9 (SD=47.6) and for the same number of samples with the highest concentration 54.8 (SD=41.41), which is statistically not significant (Mann-Whitney Rank Sum test, p=0.121). If only eight samples with highest and lowest oocyst concentration were tested (28 pairwise distance values for each group), the distances between the high concentration samples are significantly smaller (Mann-Whitney Rank Sum test p=0.015).

260   As for the taxonomy analysis described above, we conclude from these results that proliferation of *C. parvum* leads to a convergence of the inferred bacterial metagenome.

As described above for the taxonomy analysis, LEfSe was used to identify KEGG pathways which differ significantly in abundance between the 10 samples from highly infected and the same number of samples from lightly infected mice. Underscoring the difference at the

265   metagenome level between fecal samples from severely and mildly infected mice, 22 of 39 KEGG level 2 pathways were significantly different between the two groups (Table S1). In comparison to the severely infected mice, the microbiota of mild infections was characterized by a high abundance of pathways related to replication, such as carbohydrate, amino acid and nucleic acid metabolism. These results extend the taxonomy presented in Fig. 4, suggesting that

270   the mouse dysbiotic cryptosporidiosis metagenome is selected for other functions than bacterial replication.

Discussion

In a comprehensive review of the literature, Kristensen et al. (*30*) found a small number of

275   publications describing randomized controlled probiotics trials which included the

characterization of fecal microbiota. The surprising conclusion of this survey is that no

publications reported a significant change in the microbiota based on OTU richness, evenness or

diversity analysis. Although our experiments were not designed to assess the probiotics' impact

on the microbiota, we did find a significant probiotic effect. However, as no uninfected groups

280   treated with probiotics were included, the change in microbiota profile could be related to the

severity of cryptosporidiosis rather than a direct impact of consumption of probiotics. Our focus

was not to model the impact of probiotics on the gut ecosystem, but to assess whether probiotics

can mitigate the severity of cryptosporidiosis.

As we do not observe a significant increase in probiotic bacteria in the feces of treated

285   mice, we postulate that some of the bacterial or prebiotic ingredients present in the probiotic

product induced changes in the mouse intestinal environment favoring the proliferation of *C.*

parvum. Proliferation of the parasite then leads to extensive secondary modifications of the

microbiota which were detected by 16S amplicon sequencing. An impact of the prebiotics

present in the product, acacia gum, larch gum, oligosaccharides and L-glutamine, on the

290   microbiota cannot be excluded. Elucidating the mechanism by which probiotic administration

promotes proliferation of *C. parvum* will require testing of individual probiotic species or

defined combinations of species and/or prebiotics (*31*) and metabolomics analysis to identify

potential mediators of the probiotics effect. This research is of primary importance to enable

targeted manipulations of the microbiota aimed at limiting proliferation of *Cryptosporidium*

295   parasites. Zhu et al. (*19*) describe methods to "edit" the gut microbiota, in this case by inhibiting

the multiplication of facultative anaerobes. An analogous approach could be used to investigate

the causal link between parasite proliferation and dysbiosis. Although mice infected with *C. parvum* do not develop diarrhea, the fecal microbiota from heavily infected animals in our experiments resembles the fecal microbiota of humans suffering from cholera diarrhea (*26-28*) or

300 diarrhea of other etiologies (*28*), indicating that neither pathogen type nor fecal water content are important to change the microbiota. A characteristic of many intestinal pathologies of infectious or other causes is an increase in the proportion of Gammaproteobacteria (*32*). Although exceptions to this trend have been reported (*33*), a shift towards facultative anaerobes reflecting increased permeability of the gut epithelium is a hallmark of infectious (*26, 27, 34, 35*),

305 inflammatory (*36-38*) and other intestinal pathologies (*39*). The abundance of Gammaproteobacteria in the distal gut of mice heavily infected with *C. parvum* is significant because it indicates a shift in the luminal oxygen gradient (*40*) creating conditions favoring multiplication of Gammaproteobacteria. Thus, even in the absence of diarrhea, the mouse is a valuable model of cryptosporidiosis pathology. The observed abundance of facultative anaerobes

310 in the absence of diarrhea also demonstrates that diarrhea is not a direct cause of dysbiosis. Previous observations showing that cryptosporidiosis impacts the murine microbiota in the absence of any specific treatment (*18*) is consistent with dysbiosis being a consequence of the infection, perhaps caused by epithelium erosion, villus atrophy (*41-43*), increased sloughing of epithelial cells and a resulting increase in luminal O_2. These observations raise the question

315 whether *Cryptosporidium* proliferation responds to oxygen concentration in the gut lumen. Although the proliferative stages of the parasite are intracellular, sporozoites, merozoites and microgametes are extracellular. Selective inhibition or promotion of oxygen-consuming bacteria (*19*) to temporarily raise or deplete luminal O_2 (*20*) could potentially be investigated to assess the

response of *C. parvum* and explore indirect approaches to mitigating the severity and duration of

320   cryptosporidiosis through microbiota manipulation.

Few studies have reported on the effect of diet on *C. parvum* infection. Liu et al. (*44*)

found that protein deficiency increases the concentration of *C. parvum* DNA in feces. However,

the difference between normal and protein-deficient animals was reported at 20 h post-infection.

Since *C. parvum* is not known to complete its life cycle in less than 72 h (*45*), the diet effect is

325   difficult to interpret. A second study found a positive effect of pomegranate extract on

cryptosporidiosis in calves (*46*). The authors report that calves fed milk supplemented with

extract excreted fewer oocysts. The very limited range of the literature on the effects of diet on

cryptosporidiosis illustrates the need for additional research, particularly basic research on

mechanistic aspects of parasite-microbiota interaction. The possibility of including the innate and

330   adaptive immune response in this research is currently limited by the fact that studies in mice

infected with *C. parvum* require immune suppression.

Although the results of experiment 1 and experiment 2 are consistent, differences were

also noticed. Most notably, average oocyst output in experiment 2 was higher, indicative of a

more severe infection. Corroborating the model discussed above, more severe infections were

335   associated with higher relative abundance of Gammaproteobacteria (Fig. 4). The reason for the

difference between severity of infection is hard to determine, but the different route of

dexamethasone administration mentioned above could have contributed to this outcome. The use

of two *C. parvum* isolates is unlikely to be a relevant factor as MD and TU114 are not known to

differ with respect to their virulence phenotype in dexamethasone treated mice (unpublished

340   observations). Differences in fecal oocyst output between co-housed mice was also observed

(Fig. 1). As described in Materials and Methods, animals from a same cage were housed

individually only for 16 h three times a week for collection of feces, but were otherwise housed together in two cages per treatment or 4 cages for each experiment. The difference in oocyst output and microbiota profile between cagemates is difficult to explain given the close contact

345   between animals. This phenomenon justifies mice to be sampled individually, rather than sampling by group as is common practice.

Conclusions

In the absence of effective anti-protozoal drugs to control cryptosporidiosis, alternative treatments are attractive. However, our current understanding of how microbiota perturbation,

350   whether induced by diet, pro-, anti- or prebiotics, affects enteric pathogens including *Cryptosporidium* is very incomplete. Identifying specific mechanisms impacting pathogen virulence in response to probiotics consumption or diet may enable the development of targeted microbiota editing measures to mitigate the severity of cryptosporidiosis. Methods designed to detect metabolome modifications (*47*) will be needed to supplement the information gained from

355   16S amplicon sequencing. Lastly, enhancing the value of the rodent cryptosporidiosis model, the observed shift towards facultative anaerobes indicates common pathogenic changes in the human and rodent intestine in response to enteric infections.

Materials and Methods

360   *Parasites*

Oocysts from *C. parvum* isolate MD (*48*) or TU114 (*49*) were used in experiment 1 and 2, respectively. MD is a zoonotic isolate, whereas TU114 belong to the anthroponotic subgroup characterized by a IIc GP60 genotype (*50*). Oocysts were purified from mouse feces on gradients

of Nycodenz (Alere Technologies, Oslo, Norway) as described (*51*). The age of the oocysts was

365   13 and 110 days for experiment 1 and 2, respectively.

Mouse experiments.

To test the effect of a commercially available probiotic, two replicate experiments were

conducted in mice. In each experiment, herein referred to as experiment 1 and experiment 2,

370   respectively, 16 female CD-1 mice approximately 6 weeks of age were used. Upon delivery,

each mouse was individually tagged and randomly assigned to one of four groups of four mice.

Mice were immunosuppressed by adding dexamethasone 21-phosphate disodium (Sigma, cat no.

D1169) to the drinking water at a concentration of 16 mg/l (*52*) starting on the day of arrival,

defined here as day -7 post-infection (PI), i.e., 7 days prior to infection. To deplete the native

375   intestinal microbiota, vancomycin and streptomycin were added to the drinking water at a

concentration of 500 mg/l and 5 g/l, respectively, starting on day -6 PI. Metronidazole at a dose

of 20 mg/kg was given daily by gavage starting on day -6 PI. The antibiotic treatment was

discontinued on day -2 PI. Starting on day -1 PI, the drinking water was supplemented with 1.3 g

of probiotic added to 500 ml water. This product contains 15 bacterial strains belonging to the

380   genera *Bifidobacter* (4 species), *Lactobacillus* (9 species) and *Streptococcus thermophilus*. In

addition to bacteria, 1 g of product contains 8 mg Acacia gum, 540 mg Larch gum, 115 mg

galactooligosaccharide, 212 mg L-glutamine and 150 IU vitamin D3. When dissolved into 500

ml of water, the final concentration of these ingredients was 20 μg/ml, 1.4 mg/ml, 0.3 mg/ml,

0.55 mg/ml and 0.4 IU/ml, respectively. The product is flavorless. Drinking water with

385   dexamethasone and probiotic water was replaced every 3 days. Mice were orally infected on day

0 PI with approximately 5×10^4 *C. parvum* oocysts. In experiment 1, to compensate for

increased water uptake in the two groups receiving probiotic, the concentration of

dexamethasone phosphate in the water of the two treated groups was reduced to 10 mg/l starting

on day 10 PI. In experiment 2, to avoid possible differences in dexamethasone uptake with

390   drinking water, the drug (Dexamethasone; Sigma, cat no. D1756) was given only subcutaneously

every second day starting on day 2 PI. A volume of 100 µl of 10 mg/ml dexamethasone

suspension was injected alternatively into the right and left side of the abdomen. To obtain fecal

pellets for microbiota analysis, mice were individually transferred to a 1-liter plastic beaker and

pellets collected upon defecation. Pellets were stored at -20°C. To collect feces for oocyst

395   enumeration, mice were individually transferred overnight to collection cages fitted with a wire

bottom. Feces were collected from these cages were stored at 4°C. In the morning, mice were

returned to their respective group cage, such that they were housed individually for 14-16 h on

the days when feces for oocyst enumeration were collected. While in conventional cages, the

mice were always housed with the same cagemates.

400   Animal experiments adhered to the NIH Guide for the Care and Use of Laboratory

Animals and were approved by the Tufts University Animal Care and Use Committee.

Enumeration of oocysts.

Feces collected overnight were weighted, diluted 1:5 in distilled water and homogenized with a

405   vortex. To remove debris, fecal homogenates were filtered through 100 µm cell strainers

(Corning cat. no. 431752) by centrifugation at 1300 x g. The filtrates were homogenized and

volumes of 1 ml centrifuged at 6700 x g for 5 min. The supernatant was discarded and the pellet

was suspended in 500 µl of PBS supplemented with 10% fetal bovine serum. A volume of 20 µl

of this suspension was transferred to a 1.5 ml microcentrifuge tube and 20 µl of a 1:5 dilution of

410   monoclonal antibody 5F10 cell culture supernatant. This antibody reacts specifically with the *Cryptosporidium* oocyst wall without binding to other parasite antigens (Sheoran, unpublished observation). Samples were incubated for 30 min at room temperature. Following incubation with primary antibody, the samples were centrifuged for 10 min at 6700 x g, the pellet washed once in 500 µl of PBS with 10% FBS and incubated with 20 µl of secondary antibody (Alexa

415   Fluor 488 goat IgG anti-mouse) for 30 min at room temperature. After incubation, 500 µl of PBS was added and the samples washed once in PBS. For each experiment five samples were randomly selected for replication. Replication involved processing and labelling 5 separate aliquots originating from each strained and washed sample. Labelled samples were analyzed by flow cytometry using a Becton Dickinson Accuri C6 cytometer. Distance matrices were

420   calculated in GenAlEx 6.5 (*53*) based on the pairwise difference between oocyst concentrations. Specifically, the distance between sample A containing an oocyst concentration of x_a/g feces and sample B containing a concentration of x_b/g feces was calculated as $(x_a - x_b)^2$. The accuracy of the flow cytometry oocyst enumeration method was evaluated by correlating the counts against the *Cryptosporidium* 18S ribosomal RNA gene copy number estimated using real-time PCR with

425   published primers (*54*). This analysis based on five randomly chosen experiment 1 samples generated a correlation coefficient of 69%.

Microbiota analysis.

DNA was extracted from 10 mg of feces collected individually from each mouse. DNA was

430   extracted in a QIACube instrument using the QIAamp PowerFecal DNA kit (QIAGEN, cat. 12830-50) according to manufacturer's protocol. DNA was eluted in 50 µl of elution buffer and stored at -20°C. A previously described PCR protocol to prepare 16S V1V2 amplicons libraries

for high-throughput sequencing was used (*18*). The only deviation from this procedure was the downstream primer; instead of canonical primer 338R we used primer Bac R V2 short

435   (GTTCAGACGTGTGCTCTTCCGATCtgctgcctcccgtaggagt), where the lowercase characters are equivalent to the conserved 338R sequence (*55*). One microliter of primary PCR reaction was subjected to a secondary PCR to incorporate a 6-nucleotide barcode using to each sample. The secondary amplification was as described (*18*), except that downstream primer

*CAAGCAGAAGACGGCATACGAGAT*nnnnnnGTGACTGGAGTTCAGACGTGTGCTCTTCC

440   was used. The italicized nucleotides represent the Illumina adaptor and the lowercase characters the barcode unique to each sample. To assess the quality of the PCRs, a portion of the amplification product was electrophoresed on 1.5% agarose and visualized using GelRed™ (Biotium). The concentration of each final amplicon was measured in a Qbit spectrophotomer and up to 80 amplicons pooled at approximately equal concentration. The pooled library was size

445   selected with a Pippin HT library size selection system (Sage BioScience). Libraries were sequenced in an Illumina MiSeq sequencer at Tufts University Genomics core (tucf.org) using single-end 300-nucleotide strategy. To control for technical variation introduced during library preparation and sequencing, each library included two replicates of two randomly chosen samples. Replication involved the processing of duplicate fecal samples processed, amplified and

450   barcoded individually.

Bioinformatics.

FASTQ formatted sequences were processed using programs found in mothur (*56*) essentially as described (*18*). Briefly, random subsamples of 5000 sequences per sample were processed. This

455   procedure is not expected to bias the analysis (*57*) since the number of sequences per barcode

was relatively constant. The mean number of sequences per sample in experiment 1 was 1.03 x

10^5 (SD=2.44 x 10^4). In experiment 2 the average number of reads was 1.01 x 10^5 (SD=3.22 x

10^4), representing a coefficient of variation of 0.23 and 0.31, respectively. V1V2 sequences

were trimmed to 200 nucleotides to eliminate 3′ sequence with a mean Phred quality score <30.

460   Sequences were aligned and sequences with the following properties were removed: sequences

that did not align, sequences with ambiguous base calls and sequences with homopolymers >8

nt. To further reduce the number of putative sequence errors, program *pre.cluster* was used to

merge unique sequences differing by one nucleotide position with the majority sequence (*58*).

This sequence curation protocol removed 15,748 from 400,000 experiment 1 sequences (3.9%)

465   and 21,546 from 355,000 experiment 2 sequences (6.0%) sequences. Pairwise UniFrac

phylogenetic distances (*22*) between samples were calculated in *mothur*. Analysis of Similarity

(ANOSIM) (*59*) was used to test the significance of clustering by treatment. Program *anosim*

was run in *mothur* using a weighted UniFrac distance matrix as input. Operational Taxonomic

Units (OTUs) were obtained using program *cluster*, also found in *mothur*, using the OptiClust

470   clustering method (*60*) and a distance cut-off of 3%.

Linear Discriminant Analysis as implemented in program LEfSe (*24*) was used to

identify statistically significant differences in OTU abundance profiles between two groups of

samples defined indepently of treatment as heavily and lightly infected. Heavy and light

infection was defined on the basis of fecal oocyst concentration determined by flow cytometry as

475   described above. In the experiment-wide LefSe analyses, the 10 samples with the highest oocyst

concentration and the 10 samples with the lowest oocyst concentration were selected. When

analyzing subsamples of probiotic and control mice separately, the five samples with the highest

oocyst concentration and the same number of samples with the lowest oocyst concentration were tested using LEfSe (*24*).

480   Redundancy Analysis (RDA) was used to test the significance of association between OTU profile and oocyst concentration or between KEGG function profile and oocyst concentration. The program was run in CANOCO (*25*). OTU abundance values for the 100 most abundant OTUs, or KEGG functions (n=39) inferred with metagenome prediction tool PICRUSt (*29*) served as dependent variables. Oocyst concentration determined by flow cytometry as

485   described above served as the independent variable. Pairwise distance between KEGG profiles was calculated as described above for oocyst concentration, except that the squared difference was summed over all KEGG categories. This metric is equivalent to the square of the Euclidean distance.

Correlation between pairs of matrices was tested with the Mantel test (*61*). This test uses

490   random permutation of the elements in one matrix to detect a relationship between the elements of two matrices (*62*). The implementation of Mantel in GenAlEx 6.5 (*53*) was used.

16S sequence data from experiment 1 and experiment 2 were deposited in the ENA Sequence Read Archive under study accession number PRJEB25162 and PRJEB25164, respectively.

495

References

1. P. A. Rochelle, G. D. Di Giovanni, in *Cryptosporidium: parasite and disease*. (Springer, 2014), pp. 489-513.

2. S. M. Cacciò, L. Putignani, in *Cryptosporidium: parasite and disease*. (Springer, 2014), pp.

500   43-79.

3.   S. M. Mor, J. K. Tumwine, G. Ndeezi, M. G. Srinivasan, D. H. Kaddu-Mulindwa, S.

Tzipori, J. K. Griffiths, Respiratory cryptosporidiosis in HIV-seronegative children in

Uganda: potential for respiratory transmission. *Clin Infect Dis* **50**, 1366-1372 (2010).

4.   K. L. Kotloff, J. P. Nataro, W. C. Blackwelder, D. Nasrin, T. H. Farag, S. Panchalingam, Y.

505   Wu, S. O. Sow, D. Sur, R. F. Breiman, A. S. Faruque, A. K. Zaidi, D. Saha, P. L. Alonso, B.

Tamboura, D. Sanogo, U. Onwuchekwa, B. Manna, T. Ramamurthy, S. Kanungo, J. B.

Ochieng, R. Omore, J. O. Oundo, A. Hossain, S. K. Das, S. Ahmed, S. Qureshi, F. Quadri,

R. A. Adegbola, M. Antonio, M. J. Hossain, A. Akinsola, I. Mandomando, T. Nhampossa, S.

Acacio, K. Biswas, C. E. O'Reilly, E. D. Mintz, L. Y. Berkeley, K. Muhsen, H. Sommerfelt,

510   R. M. Robins-Browne, M. M. Levine, Burden and aetiology of diarrhoeal disease in infants

and young children in developing countries (the Global Enteric Multicenter Study, GEMS):

a prospective, case-control study. *Lancet* **382**, 209-222 (2013).

5.   J. A. Harp, W. Chen, A. G. Harmsen, Resistance of severe combined immunodeficient mice

to infection with Cryptosporidium parvum: the importance of intestinal microflora. *Infect*

515   *Immun* **60**, 3509-3512 (1992).

6.   J. A. Harp, Cryptosporidium and host resistance: historical perspective and some novel

approaches. *Animal Health Research Reviews* **4**, 53-62 (2003).

7.   S. Lacroix-Lamande, W. Guesdon, F. Drouet, L. Potiron, L. Lantier, F. Laurent, The gut

flora is required for the control of intestinal infection by poly(I:C) administration in

520   neonates. *Gut Microbes* **5**, 533-540 (2014).

8.   L. Lantier, F. Drouet, W. Guesdon, R. Mancassola, C. Metton, R. Lo-Man, C. Werts, F.

Laurent, S. Lacroix-Lamande, Poly(I:C)-induced protection of neonatal mice against

intestinal Cryptosporidium parvum infection requires an additional TLR5 signal provided by the gut flora. *J Infect Dis* **209**, 457-467 (2014).

525   9.   S. K. Gorla, N. N. McNair, G. Yang, S. Gao, M. Hu, V. R. Jala, B. Haribabu, B. Striepen, G. D. Cuny, J. R. Mead, L. Hedstrom, Validation of IMP dehydrogenase inhibitors in a mouse model of cryptosporidiosis. *Antimicrob Agents Chemother* **58**, 1603-1614 (2014).

10.   G. A. Preidis, D. M. Saulnier, S. E. Blutt, T. A. Mistretta, K. P. Riehle, A. M. Major, S. F. Venable, M. J. Finegold, J. F. Petrosino, M. E. Conner, J. Versalovic, Probiotics stimulate

530   enterocyte migration and microbial diversity in the neonatal mouse intestine. *FASEB J* **26**, 1960-1969 (2012).

11.   D. M. Rodrigues, A. J. Sousa, K. C. Johnson-Henry, P. M. Sherman, M. G. Gareau, Probiotics are effective for the prevention and treatment of Citrobacter rodentium-induced colitis in mice. *J Infect Dis* **206**, 99-109 (2012).

535   12.   T. D. Lawley, S. Clare, A. W. Walker, M. D. Stares, T. R. Connor, C. Raisen, D. Goulding, R. Rad, F. Schreiber, C. Brandt, L. J. Deakin, D. J. Pickard, S. H. Duncan, H. J. Flint, T. G. Clark, J. Parkhill, G. Dougan, Targeted restoration of the intestinal microbiota with a simple, defined bacteriotherapy resolves relapsing Clostridium difficile disease in mice. *PLoS Pathog* **8**, e1002995 (2012).

540   13.   K. K. Kondepudi, P. Ambalam, P. H. Karagin, I. Nilsson, T. Wadstrom, A. Ljungh, A novel multi-strain probiotic and synbiotic supplement for prevention of Clostridium difficile infection in a murine model. *Microbiol Immunol* **58**, 552-558 (2014).

14.   C. Colenutt, S. M. Cutting, Use of Bacillus subtilis PXN21 spores for suppression of Clostridium difficile infection symptoms in a murine model. *FEMS Microbiol Lett* **358**, 154-

545   161 (2014).

15. C. G. Buffie, V. Bucci, R. R. Stein, P. T. McKenney, L. Ling, A. Gobourne, D. No, H. Liu, M. Kinnebrew, A. Viale, E. Littmann, M. R. van den Brink, R. R. Jenq, Y. Taur, C. Sander, J. R. Cross, N. C. Toussaint, J. B. Xavier, E. G. Pamer, Precision microbiome reconstitution restores bile acid mediated resistance to Clostridium difficile. *Nature* **517**, 205-208 (2015).

550   16. Z. Liu, W. Liu, C. Ran, J. Hu, Z. Zhou, Abrupt suspension of probiotics administration may increase host pathogen susceptibility by inducing gut dysbiosis. *Scientific reports* **6**, 23214 (2016).

17. J. K. Spinler, A. Brown, C. L. Ross, P. Boonma, M. E. Conner, T. C. Savidge, Administration of probiotic kefir to mice with Clostridium difficile infection exacerbates

555   disease. *Anaerobe* **40**, 54-57 (2016).

18. R. Ras, K. Huynh, E. Desoky, A. Badawy, G. Widmer, Perturbation of the intestinal microbiota of mice infected with Cryptosporidium parvum. *Int J Parasitol* **45**, 567-573 (2015).

19. W. Zhu, M. G. Winter, M. X. Byndloss, L. Spiga, B. A. Duerkop, E. R. Hughes, L. Buttner,

560   E. de Lima Romao, C. L. Behrendt, C. A. Lopez, L. Sifuentes-Dominguez, K. Huff-Hardy, R. P. Wilson, C. C. Gillis, C. Tukel, A. Y. Koh, E. Burstein, L. V. Hooper, A. J. Baumler, S. E. Winter, Precision editing of the gut microbiota ameliorates colitis. *Nature* **553**, 208-211 (2018).

20. M. S. Kao, S. Huang, W. L. Chang, M. F. Hsieh, C. J. Huang, R. L. Gallo, C. M. Huang,

565   Microbiome precision editing: Using PEG as a selective fermentation initiator against methicillin-resistant Staphylococcus aureus. *Biotechnol J* **12**, (2017).

21. C. M. Theriot, Beyond Structure: Defining the Function of the Gut Using Omic Approaches for Rational Design of Personalized Therapeutics. *mSystems* **3**, (2018).

22. C. Lozupone, M. Hamady, R. Knight, UniFrac - an online tool for comparing microbial
community diversity in a phylogenetic context. *BMC Bioinformatics* **7**, 371-385 (2006).

23. K. M. Keeney, S. Yurist-Doutsch, M. C. Arrieta, B. B. Finlay, Effects of antibiotics on
human microbiota and subsequent disease. *Annu Rev Microbiol* **68**, 217-235 (2014).

24. N. Segata, J. Izard, L. Waldron, D. Gevers, L. Miropolsky, W. S. Garrett, C. Huttenhower,
Metagenomic biomarker discovery and explanation. *Genome Biol* **12**, R60 (2011).

25. C. t. Braak, P. Šmilauer, CANOCO reference manual and CanoDraw for Windows user's
guide: software for canonical community ordination (version 4.5). *Microcomputer Power,
Ithaca, New York*, (2002).

26. L. A. David, A. Weil, E. T. Ryan, S. B. Calderwood, J. B. Harris, F. Chowdhury, Y. Begum,
F. Qadri, R. C. LaRocque, P. J. Turnbaugh, Gut microbial succession follows acute secretory
diarrhea in humans. *MBio* **6**, e00381-00315 (2015).

27. S. Monira, S. Nakamura, K. Gotoh, K. Izutsu, H. Watanabe, N. H. Alam, T. Nakaya, T.
Horii, S. I. Ali, T. Iida, M. Alam, Metagenomic profile of gut microbiota in children during
cholera and recovery. *Gut pathogens* **5**, 1 (2013).

28. M. Pop, A. W. Walker, J. Paulson, B. Lindsay, M. Antonio, M. A. Hossain, J. Oundo, B.
Tamboura, V. Mai, I. Astrovskaya, H. Corrada Bravo, R. Rance, M. Stares, M. M. Levine,
S. Panchalingam, K. Kotloff, U. N. Ikumapayi, C. Ebruke, M. Adeyemi, D. Ahmed, F.
Ahmed, M. T. Alam, R. Amin, S. Siddiqui, J. B. Ochieng, E. Ouma, J. Juma, E. Mailu, R.
Omore, J. G. Morris, R. F. Breiman, D. Saha, J. Parkhill, J. P. Nataro, O. C. Stine, Diarrhea
in young children from low-income countries leads to large-scale alterations in intestinal
microbiota composition. *Genome Biol* **15**, R76 (2014).

29. M. G. Langille, J. Zaneveld, J. G. Caporaso, D. McDonald, D. Knights, J. A. Reyes, J. C. Clemente, D. E. Burkepile, R. L. Vega Thurber, R. Knight, R. G. Beiko, C. Huttenhower, Predictive functional profiling of microbial communities using 16S rRNA marker gene sequences. *Nat Biotechnol* **31**, 814-821 (2013).

595 30. N. B. Kristensen, T. Bryrup, K. H. Allin, T. Nielsen, T. H. Hansen, O. Pedersen, Alterations in fecal microbiota composition by probiotic supplementation in healthy adults: a systematic review of randomized controlled trials. *Genome Med* **8**, 52 (2016).

31. J. J. Faith, P. P. Ahern, V. K. Ridaura, J. Cheng, J. I. Gordon, Identifying gut microbe-host phenotype relationships using combinatorial communities in gnotobiotic mice. *Sci Transl* 600 *Med* **6**, 220ra211 (2014).

32. S. E. Winter, C. A. Lopez, A. J. Baumler, The dynamics of gut-associated microbial communities during inflammation. *EMBO Rep* **14**, 319-327 (2013).

33. S. Becker-Dreps, I. Allali, A. Monteagudo, S. Vilchez, M. G. Hudgens, E. T. Rogawski, I. M. Carroll, L. E. Zambrana, F. Espinoza, M. A. Azcarate-Peril, Gut Microbiome 605 Composition in Young Nicaraguan Children During Diarrhea Episodes and Recovery. *Am J Trop Med Hyg* **93**, 1187-1193 (2015).

34. A. Hsiao, A. M. Ahmed, S. Subramanian, N. W. Griffin, L. L. Drewry, W. A. Petri, Jr., R. Haque, T. Ahmed, J. I. Gordon, Members of the human gut microbiota involved in recovery from Vibrio cholerae infection. *Nature* **515**, 423-426 (2014).

610 35. N. R. Barash, J. G. Maloney, S. M. Singer, S. C. Dawson, Giardia Alters Commensal Microbial Diversity throughout the Murine Gut. *Infect Immun* **85**, (2017).

36. I. Mukhopadhya, R. Hansen, E. M. El-Omar, G. L. Hold, IBD-what role do Proteobacteria play? *Nat Rev Gastroenterol Hepatol* **9**, 219-230 (2012).

37. P. M. Munyaka, M. F. Rabbi, E. Khafipour, J. E. Ghia, Acute dextran sulfate sodium (DSS)-induced colitis promotes gut microbial dysbiosis in mice. *J Basic Microbiol* **56**, 986-998 (2016).

38. C. C. Gillis, E. R. Hughes, L. Spiga, M. G. Winter, W. Zhu, T. Furtado de Carvalho, R. B. Chanin, C. L. Behrendt, L. V. Hooper, R. L. Santos, S. E. Winter, Dysbiosis-Associated Change in Host Metabolism Generates Lactate to Support Salmonella Growth. *Cell Host Microbe* **23**, 54-64 e56 (2018).

39. O. Manor, R. Levy, C. E. Pope, H. S. Hayden, M. J. Brittnacher, R. Carr, M. C. Radey, K. R. Hager, S. L. Heltshe, B. W. Ramsey, S. I. Miller, L. R. Hoffman, E. Borenstein, Metagenomic evidence for taxonomic dysbiosis and functional imbalance in the gastrointestinal tracts of children with cystic fibrosis. *Scientific reports* **6**, 22493 (2016).

40. M. G. Espey, Role of oxygen gradients in shaping redox relationships between the human intestine and its microbiota. *Free Radic Biol Med* **55**, 130-140 (2013).

41. S. Tzipori, W. Rand, J. Griffiths, G. Widmer, J. Crabb, Evaluation of an animal model system for cryptosporidiosis: therapeutic efficacy of paromomycin and hyperimmune bovine colostrum-immunoglobulin. *Clin Diagn Lab Immunol* **1**, 450-463 (1994).

42. R. A. Argenzio, J. A. Liacos, M. L. Levy, D. J. Meuten, J. G. Lecce, D. W. Powell, Villous atrophy, crypt hyperplasia, cellular infiltration, and impaired glucose-Na absorption in enteric cryptosporidiosis of pigs. *Gastroenterology* **98**, 1129-1140 (1990).

43. J. Vitovec, B. Koudela, Pathogenesis of intestinal cryptosporidiosis in conventional and gnotobiotic piglets. *Vet Parasitol* **43**, 25-36 (1992).

635   44. J. Liu, D. T. Bolick, G. L. Kolling, Z. Fu, R. L. Guerrant, Protein Malnutrition Impairs Intestinal Epithelial Cell Turnover, a Potential Mechanism of Increased Cryptosporidiosis in a Murine Model. *Infect Immun* **84**, 3542-3549 (2016).

45. W. L. Current, T. B. Haynes, Complete development of Cryptosporidium in cell culture. *Science* **224**, 603-605 (1984).

640   46. S. Weyl-Feinstein, A. Markovics, H. Eitam, A. Orlov, M. Yishay, R. Agmon, J. Miron, I. Izhaki, A. Shabtay, Short communication: effect of pomegranate-residue supplement on Cryptosporidium parvum oocyst shedding in neonatal calves. *Journal of dairy science* **97**, 5800-5805 (2014).

47. J. K. Jansson, E. S. Baker, A multi-omic future for microbiome studies. *Nat Microbiol* **1**,
645   16049 (2016).

48. P. C. Okhuysen, S. M. Rich, C. L. Chappell, K. A. Grimes, G. Widmer, X. C. Feng, S. Tzipori, Infectivity of a Cryptosporidium parvum isolate of cervine origin for healthy adults and interferon-gamma knockout mice. *Journal of Infectious Diseases* **185**, 1320-1325 (2002).

650   49. G. Widmer, Y. Lee, P. Hunt, A. Martinelli, M. Tolkoff, K. Bodi, Comparative genome analysis of two Cryptosporidium parvum isolates with different host range. *Infect Genet Evol* **12**, 1213-1221 (2012).

50. M. E. Mallon, A. MacLeod, J. M. Wastling, H. Smith, A. Tait, Multilocus genotyping of Cryptosporidium parvum Type 2: population genetics and sub-structuring. *Infect Genet Evol*
655   **3**, 207-218 (2003).

51. G. Widmer, X. Feng, S. Tanriverdi, Genotyping of Cryptosporidium parvum with microsatellite markers. *Methods Mol Biol* **268**, 177-187 (2004).

52. S. Yang, M. C. Healey, The immunosuppressive effects of dexamethasone administered in drinking water to C57BL/6N mice infected with Cryptosporidium parvum. *J Parasitol* **79**, 626-630 (1993).

53. R. Peakall, P. E. Smouse, GenAlEx 6.5: genetic analysis in Excel. Population genetic software for teaching and research--an update. *Bioinformatics* **28**, 2537-2539 (2012).

54. S. E. Stroup, S. Roy, J. McHele, V. Maro, S. Ntabaguzi, A. Siddique, G. Kang, R. L. Guerrant, B. D. Kirkpatrick, R. Fayer, J. Herbein, H. Ward, R. Haque, E. R. Houpt, Real-time PCR detection and speciation of Cryptosporidium infection using Scorpion probes. *J Med Microbiol* **55**, 1217-1222 (2006).

55. G. C. Baker, J. J. Smith, D. A. Cowan, Review and re-analysis of domain-specific 16S primers. *J Microbiol Methods* **55**, 541-555 (2003).

56. P. D. Schloss, S. L. Westcott, T. Ryabin, J. R. Hall, M. Hartmann, E. B. Hollister, R. A. Lesniewski, B. B. Oakley, D. H. Parks, C. J. Robinson, J. W. Sahl, B. Stres, G. G. Thallinger, D. J. Van Horn, C. F. Weber, Introducing mothur: open-source, platform-independent, community-supported software for describing and comparing microbial communities. *Appl Environ Microbiol* **75**, 7537-7541 (2009).

57. P. J. McMurdie, S. Holmes, Waste not, want not: why rarefying microbiome data is inadmissible. *PLoS Comput Biol* **10**, e1003531 (2014).

58. S. M. Huse, D. M. Welch, H. G. Morrison, M. L. Sogin, Ironing out the wrinkles in the rare biosphere through improved OTU clustering. *Environ Microbiol* **12**, 1889-1898 (2010).

59. K. R. Clarke, Nonparametric Multivariate Analyses of Changes in Community Structure. *Aust J Ecol* **18**, 117-143 (1993).

680   60.   S. L. Westcott, P. D. Schloss, OptiClust, an Improved Method for Assigning Amplicon-Based Sequence Data to Operational Taxonomic Units. *mSphere* **2**, (2017).

61.   N. Mantel, The detection of disease clustering and a generalized regression approach. *Cancer Res* **27**, 209-220 (1967).

62.   P. E. Smouse, J. C. Long, R. R. Sokal, Multiple regression and correlation extensions of the

685   Mantel test of matrix correspondence. *Systematic zoology* **35**, 627-632 (1986).

Figures

Fig. 1 Effect of probiotic on severity of *C. parvum* cryptosporidiosis in immune-suppressed mice. The graphs show normalized oocyst counts expressed as oocysts/g feces for two

695   independent experiments. Each line represents one mouse. Error bars show SD based on five replicate counts of selected samples.

Fig. 2. Impact of probiotic on the fecal microbiome of *C. parvum* infected mice. Principal Coordinate Analysis was used to display weighted UniFrac distances between pairs of fecal microbiome samples. Experiment 1 analysis (left) includes data from 64 fecal samples collected

700   from day 5 of treatment (day 4 PI) until day 16 of treatment (day 15 PI). For experiment 2, 55 samples were analyzed. Each datapoint represents one sample, color-coded according to treatment and group as shown in Fig. 1. Matching triangle symbols indicate replicate analyses of the same fecal samples.

Fig. 3 Oocyst output is unrelated to diversity of bacterial microbiome. Oocyst output normalized

705   for feces volume was plotted against Shannon diversity for 44 samples collected on three days

which were analyzed for both properties in experiment 1 and 53 samples from experiment 2.

Color indicates experimental group as described in Fig. 1. Samples were collected from

individual mice.

Fig. 4 Taxonomy of fecal microbiome from heavily and lightly infected mice shows that heavy

710   infections are associated with increased abundance of Proteobacteria. For each experiment,

bacterial taxa significantly associated with severity of infection were identified using LEfSe (24)

in a comparison of ten samples with the highest (high) and lowest (low) oocyst concentration;

twenty samples were included for each experiment. Color indicates phylum and color intensity

genus or highest taxonomic level (family, order etc.) identified; green Proteobacteria; red,

715   Firmicutes; blue, Actinobacteria.
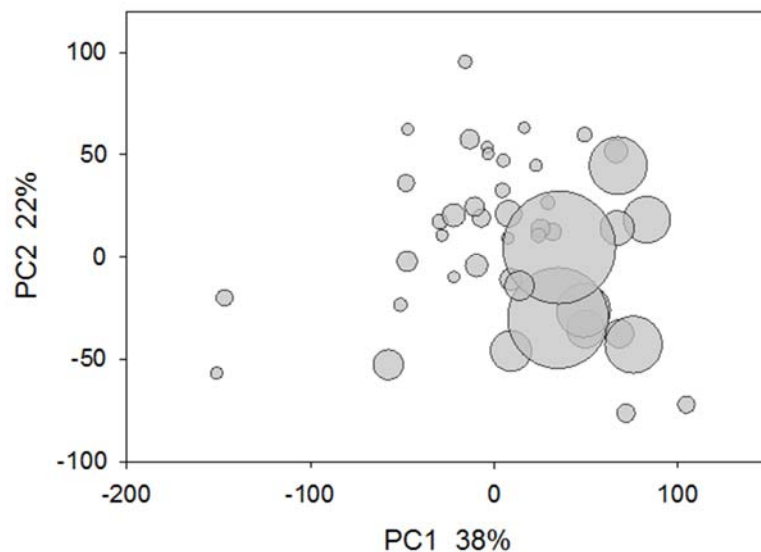
Supplementary materials

720

Fig. S1. Principal Coordinates Analysis based on KEGG level 2 functional categories. Datapoints located in close proximity have similar metagenomes. The size of the circles is proportional to oocyst concentration. Metagenome gene abundance from experiment 2 was inferred from 16S sequence data using PICRUSt for 44 fecal samples analyzed by 16S amplicon sequencing and oocyst concentration.

725

Table S1 Metagenomic differences grouped by KEGG level 2 pathways between severely infected and mildly infected mice.

730

Group	KEGG pathway	log(abundance)	LDA score	p
Severely infected	Poorly Characterized	4.704	2.80	0.034
	Cellular Processes and Signaling	4.629	3.23	0.001
	Metabolism of Cofactors and Vitamins	4.592	2.96	0.041
	Cell Motility	4.540	3.59	0.001
	Genetic Information Processing	4.466	2.92	0.010
	Metabolism unclassified	4.439	2.71	0.002
	Folding Sorting and Degradation	4.341	2.67	0.023
	Signal Transduction	4.332	3.28	0.000
	Glycan Biosynthesis and Metabolism	4.306	2.86	0.002
	Infectious Diseases	3.656	2.61	0.001
	Circulatory System	0.665	2.11	0.008
	Cardiovascular Diseases	0.148	2.60	0.008
Mildly infected	Carbohydrate Metabolism	5.039	3.59	0.005
	Amino Acid Metabolism	4.939	2.89	0.016
	Replication and Repair	4.924	3.38	0.003
	Translation	4.722	3.27	0.002
	Nucleotide Metabolism	4.586	3.04	0.005
	Lipid Metabolism	4.484	2.91	0.002
	Xenobiotics Biodegrad. & Metabolism	4.336	3.05	0.003
	Metabolism of other Amino Acids	4.200	2.53	0.028
	Cell Growth and Death	3.685	2.38	0.001
	Signaling Molecules and Interaction	3.353	2.25	0.001